Protective and Therapeutic Effect of Molsidomine on Bleomycin-Induced Lung Fibrosis in Rats

Talat Kilic,[1,6] Hakan Parlakpinar,[2] Alaadin Polat,[3] Elif Taslidere,[4] Nigar Vardi,[4] Ediz Sarihan,[5] Hilal Ermis,[1] and Kevser Tanbag[3]

Abstract—We aimed to investigate the preventive and treatment effect of molsidomine (MOL) on bleomycin (BLC)-induced lung injury in rats. Rats were assigned into groups as follows: control group; MOL group, 10 mg/kg MOL was continued orally for 29 day; BLC group, a single intra-tracheal injection of BLC (2.5 mg/kg), MOL+BLC-preventive group, 10 mg/kg MOL was administered 1 day before the intratracheal BLC injection and continued for 14 days; BLC+MOL-treatment group 10 mg/kg MOL was given on 14th day after the intratracheal BLC injection and continued until sacrifice. All animals were sacrificed on 29th day after BLC administration. The semiquantitative histopathological assessment, tissue levels of malondialdehyde (MDA), superoxide dismutase (SOD), catalase (CAT), glutathione peroxidase (GPx), reduced glutathione (GSH), total antioxidant status (TAS), total oxidant status (TOS), myeloperoxidase (MPO), and oxidative stress index (OSI) were measured. BLC-provoked histological changes were significantly detected compared to the control group. MOL restored these histological damages in different quantity in the treatment and preventive groups. BLC administration significantly decreased levels of GSH and TAS when compared to controls and these reductions was significantly ameliorated by MOL given prophylactic setting. However, therapeutic MOL administration significantly increased the TAS level decreased by BLC. The levels of MDA, MPO, and TOS were significantly increased with BLM, and these augmentations of MDA and TOS were significantly reduced by MOL given prophylactic setting. Furthermore, the OSI was higher in the BLC group, and this increase was reversed by the MOL administration before and after BLC treatment. In this study, both protective and therapeutic effects of MOL against BLC-induced lung fibrosis were demonstrated for the first time.

KEY WORDS: bleomycin; pulmonary fibrosis; inflammation; molsidomine; idiopathic pulmonary fibrosis.

INTRODUCTION

Fibroblast reproduction and extracellular matrix re-modeling characterize pulmonary fibrosis. Up to one half of the patients with pulmonary fibrosis are with idiopathic pulmonary fibrosis (IPF). IPF is defined as a chronic pro-gressive lung disease of unknown cause associated with abnormal deposition of extracellular collagen, particularly in the early stage of the disease [1]. It is characterized by aggregation of alveolar macrophages and neutrophils in the respiratory tract, parenchymal damage, and fibrosis of the alveolar walls [2]. Activated neutrophils can also release myeloperoxidase (MPO), an enzyme that interacts with H_2O_2 to form the highly toxic hydroxyl radicals [3]. In this respect, it is logical to hypothesize that the alveolar epithe-lial cell damage that characterizes IPF may result, at least partially, from an advanced oxidant load that may have been in the lower respiratory tract of the patients. Fortu-nately, despite of intensive researches, IPF has no potent treatment other than pirfenidone, which is only obtainable

[1] Department of Pulmonary Medicine, Inonu University School Medicine, Malatya, Turkey

[2] Department of Pharmacology, Inonu University School Medicine, Malatya, Turkey

[3] Department of Physiology, Inonu University School Medicine, Malatya, Turkey

[4] Department of Embryology and Histology, Inonu University School Medicine, Malatya, Turkey

[5] Department of Emergency Medicine, Inonu University School Medicine, Malatya, Turkey

[6] To whom correspondence should be addressed at Department of Pulmonary Medicine, Inonu University School Medicine, Malatya, Turkey. E-mail: talatkilic2013@gmail.com

in Japan, Canada, and Europe, for the treatment of this disease. If lung transplantation was not performed, 80 % of these patients are lost within 5 years [4]. Hence, treating patients with agents that have anti-inflammatory, antioxidants, and antifibrotic properties as an adjuvant or neoadjuvant therapy, may have useful effects in prevention or treatment of IPF.

There are also some studies which tested several antioxidant agents, such as *N*-acetylcysteine [5], erdosteine [6], aminoguanidine [7], melatonin [8], ginkgo biloba [9], resveratrol [10], and dexpanthenol [11] in bleomycin (BLC)-induced lung fibrosis in rats as a prophylactic setting, and found these substances usually reduced or prevented lung fibrosis according to Aschoft's criteria and lung hydroxyproline content. However, in clinical practice, the majority of patients with IPF were diagnosed at a delayed stage of the disease. Thus, it is clear that new studies are needed to investigate the effect of the drugs in BLC-induced lung fibrosis model simulating human IPF at both early and late stages as a therapeutic model. BLC-induced lung fibrosis is commonly used as an animal model of human IPF, as intratracheal BLC application causes an inflammatory response alveolar cell damage, fibroblast proliferation, and collagen content deposition in mice [6, 8].

As a nitric oxide (NO) donor, MOL is a prodrug and a potent vasodilator that has been used widely as an antianginal agent [12]. In the liver, MOL decarboxylases enzymatically to form 3-morpholinosyndnonimine (SIN-1), which spontaneously liberates NO [13]. However, NO has an important role in the process of inflammation, tissue injury, and cell defense [14]. In many studies, MOL was shown to have antioxidant and anti-inflammatory properties [12, 15–17].

Since BLC, one of the clinically significant causative agents in pulmonary fibrosis, is widely used in murine model of human disease resembling pulmonary fibrosis [18], this study aimed to investigate the protective and therapeutic effects of MOL on lung fibrosis induced by BLC administration by using histopathological semiquantitative evaluation and oxidative stress markers in damaged lung tissue in rats.

MATERIAL AND METHODS

Study Design

This animal experimental study was designed in accordance with the ARRIVE guidelines [19]. This study

was approved by Animal Ethics Committee (reference number: 2012/A-60) and was conducted in accordance with the "Animal Welfare Act and the Guide for the Care and Use of Laboratory animals (NIH publication no. 5377-3, 1996), Animal Ethics Committee."

Animals and Groups

For this study, a total of 40 female Wistar Albino rats of 10–12 weeks of age and weighing 250–300 g were obtained from Inonu University Laboratory Animals Research Center and placed in a temperature (21 ± 2 °C)- and humidity (60 ± 5 %)-controlled room in which a 12:12 h light/dark cycle was maintained. The animals were divided into five groups each with eight rats, according to their experimental treatment as follows: (1) control group; (2) MOL group, 10 mg/kg MOL in 0.25 ml phosphate buffered saline (Molsidomine, Sigma Chemical C., St Louis, MO, USA) was continued orally (p.o.) for 29 days; (3) BLC group, a single intratracheal injection of BLC (2.5 mg/kg body weight in 0.25 ml phosphate buffered saline); (4) MOL+BLC-preventive group, 10 mg/kg MOL was administered 1 day before the intratracheal BLC injection and continued for 14 days p.o.; (5) BLC+MOL-treatment group, 10 mg/kg MOL was administered on the 14th day after intratracheal BLC injection and continued until sacrifice.

BLC-Induced Lung Fibrosis

The rats were weighted and then anesthetized with ketamine (75 mg/kg) and xylazine (5 mg/kg) i.p. followed by a single intratracheal injection of BLC hydrochloride (2.5 mg/kg body weight in 0.25-ml phosphate buffered saline (PBS); Nippon Kayaku, Japan). The control group received the same amount of intratracheal saline by the same route. All rats were sacrificed after 29 days of BLC injection. After sacrifice by an overdose of the anesthesia, the lung tissue specimens were quickly and meticulously harvested for biochemical and histopathological analysis. The right section of the lung was placed in liquid nitrogen and stored at −70 °C until assayed for thiobarbituric acid-reactive substances (TBARS), lipid peroxidation product, superoxide dismutase (SOD), catalase (CAT), glutathione peroxidase (GPx), reduced glutathione (GSH), MPO, total antioxidant status (TAS), total oxidant status (TOS) contents, and oxidative stress index (OSI); the left part of the lung was placed in formaldehyde solution for routine histopathological examination by light microscopy. The dosage of BLC and MOL were chosen depending on the previous dose–response studies that have been reported to

cause lung fibrosis and marked anti-oxidative and anti-inflammatory effects in rats, respectively [11, 12, 17].

Bronchoalveolar Lavage (BAL) Fluid

After being anesthetized, the lungs were prepared for lavage by cannulating the trachea with a blunt needle attached by a syringe. The lung lavage was obtained by washing the lung four times with 4 ml aliquots of saline through a tracheal cannula. Cell suspensions were concentrated by low-speed centrifugation, and the cell pellet was resuspended. Total and different cell counts were made in a hemocytometer.

Biochemical Analyses

Two hundred milligrams of frozen lung tissue specimens were cut into pieces on dry ice, homogenized in 1.15 % KCl buffer (1:9, w/v) using a manual glass homogenizer for approximately 5 min, and flushed with centrifugation for approximately 10 s to remove large debris. The supernatant was used for analysis.

Determination of TBARS Representing MDA Content

The TBARS contents of the homogenates were determined by TBARS [20]. Three milliliters of 1 % phosphoric acid and 1 ml 0.6 % thiobarbituric acid solution were added to 0.5 ml of plasma pipetted into a tube. The mixture was heated in boiling water for 45 min. After the mixture had cooled, the color was extracted into 4 ml of n-butanol. The absorbance was measured by a spectrophotometer (UV-1601; Shimadzu, Kyoto, Japan) at 532 nm. The amount of lipid peroxides was calculated as TBARS of lipid peroxidation. The results were expressed in nanomoles per gram (nmol/g tissue) according to a standard graph, which was prepared from the measurements of standard solutions (1,1,3,3-tetramethoxypropane).

Determination of SOD

Total (Cu-Zn and Mn) SOD (EC 1.15.1.1) activity was determined based on the method by Sun et al. [21]. The principle of the method is the inhibition of nitro blue tetrazolium (NBT) reduction by the xanthine–xanthine oxidase system as a superoxide (O_2^-) generator. One unit of SOD was defined as the enzyme amount causing 50 % inhibition in the NBT reduction rate. SOD activity was expressed as units per milligram protein (U/g protein).

Determination of CAT

CAT (EC 1.11.1.6) activity was determined with respect to Aebi's method [22]. The principle of the assay is based on the determination of the rate constant (k, $s-1$) or the H_2O_2 decomposition rate at 240 nm. Results were expressed as kilograms per gram protein (k/g protein).

Determination of GPx

Determination of GPx activity (EC 1.6.4.2) was measured by the method of Paglia and Valentine [23]. An enzymatic reaction in a tube containing NADPH, GSH, sodium azide, and glutathione reductase was initiated with the addition of H_2O_2, and the change in absorbance at 340 nm was monitored by a spectrophotometer. Activity was given in units per gram protein (U/mg protein).

Determination of GSH Content

The GSH content in the lung tissue as nonprotein sulfhydryls was analyzed following a previously described method [24]. Aliquots of tissue homogenate were mixed with distilled water and 50 % trichloroacetic acid in glass tubes and centrifuged at 3,000 rpm for 15 min. The supernatants were mixed with Tris buffer (0.4 M, pH 8.9), and 5,5′-dithiobis(2-nitrobenzoic acid (DTNB), 0.01 M) was added. After shaking the reaction mixture, its absorbance was measured at 412 nm within 5 min of the addition of DTNB against blank with no homogenate. The absorbance values were extrapolated from a glutathione standard curve and expressed as GSH (in micromoles per gram of tissue).

Determination of MPO Activity

MPO (EC 1.11.1.7) activity was determined by using a 4-aminoantipyrine/phenol solution as the substrate for MPO-mediated oxidation by H_2O_2, and change in the absorbance at 510 nm was recorded [25]. One unit of MPO activity was defined as the amount causing degradation of 1 μmol H_2O_2/min at 25 °C. The results were given in milliunits per gram of protein.

Measurement of TAS

TAS levels were determined using a novel automated colorimetric measurement method developed by Erel [26]. In this method, the hydroxyl radical, the most potent biological radical, is produced by the Fenton reaction and reacts with the colorless substrate O-dianisidine to produce the dianisyl radical, which is bright yellowish brown in color. Upon the addition of sample, the oxidative reactions

initiated by the hydroxyl radicals present in the reaction mix are suppressed by the antioxidant components of the sample, preventing the color to change and thereby providing an effective measure of the total antioxidant capacity of the sample. The assay has excellent precision values, which are lower than 3 %. The results were expressed as millimoles of trolox equivalent per liter.

Measurement of TOS

TOS was determined using a novel automated measurement method, developed by Erel [27]. Oxidants present in the sample oxidize the ferrous ion–O-dianisidine complex to ferric ion. The oxidation reaction is enhanced by glycerol molecules, which are abundantly present in the reaction medium. The ferric ion makes a colored complex with xylenol orange in an acidic medium. The color intensity, which can be measured spectrophotometrically, is related to the total amount of oxidant molecules present in the sample. The assay was calibrated with hydrogen peroxide, and the results were expressed in terms of micromoles of H_2O_2 equivalent per liter.

Measurement of OSI

The percentage ratio of TOS to TAC yields the OSI, an indicator of the degree of oxidative stress [27], calculated as OSI (arbitrary unit)=TOS (mmol H_2O_2 equivalent/l)/ TAC (mmol trolox equivalent/l). The OSI value for the lung samples was also calculated as OSI (arbitrary unit)=TOS (mmol H_2O_2 equivalent/g protein)/TAC (mmol trolox equivalent/g protein).

Histological Evaluations

At the end of the study, lungs were removed. The tissue samples were fixed in 10 % formalin and were embedded in paraffin. Tissue sections were cut at 5 μm, mounted on slides, stained with hematoxylin and eosin (H&E) for general lung structure, periodic acid Schiff (PAS) to identify alveolar macrophage, and Masson's trichrome for connective tissue. Lung injury was scored for each of the following tissue injury criteria: alveolar congestion, thickness of alveolar wall, enlarged alveoli, increase in connective tissue in parenchyma, and inflammation were scored on a scale of 0–4 (0 for normal lungs, 1 for 25 % injury involvement, 2 for 25–50 % injury involvement, 3 for 50–75 % injury involvement, and 4 for 75–100 % injury involvement). The total histology score is the sum score of all parameters. The observers were blinded to the treatment groups. Alveolar macrophages were counted in 10 microscopes under ×40 objective magnification using Leica Q Win Image Analysis System (Leica Micros Imaging Solution Ltd., Cambridge, UK). Sections were examined using a Leica DFC280 light microscope.

Statistics

For detecting even the minor effects, the required sample sizes used in this experiment were identified using statistical power analysis. The sample sizes necessary for a power of 0.80 were estimated using NCSS software. Data were analyzed using the SPSS software program for Windows, version 18.0 (SPSS Inc., Chicago, IL, USA). The normality of the distribution was confirmed using the Kolmogorov–Smirnov test. According to the results obtained from the normality test, one-way analysis of variance (ANOVA) and Kruskal–Wallis H test were used for the statistical analysis as appropriate. Multiple comparisons were carried out by Tukey's test (for homogeneous variances) after the ANOVA test. The results are expressed as mean ± standard deviation (S.D.) for TBARS, SOD, CAT, GPx, MPO, TOS, and OSI. After a significant Kruskal–Wallis H test, a Conover test was also carried out for GSH, TAS, and histopathological results. P values less than 0.05 were regarded as statistically significant. The values were given as median (min–max).

RESULTS

Histological Findings

The lungs of the rats in the control group showed normal lung structure and there were no lesions (Fig. 1a). The group treated with MOL alone was similar to that of the control group (Fig. 1b). No sign of connective tissue deposition was observed with Masson's trichrome staining methods (Fig. 1c, d), and the appearance of macrophages was normal with PAS-stained methods in the lungs of the control and MOL groups (Fig. 1e, f). However, there were considerable histological changes in lung tissues in the BLC group. Thickening of interalveolar septum and congestion of the parenchyma were seen in this group (Fig. 2a). Moreover, enlarged alveoli (Fig. 2b) and increase in connective tissue (Fig. 2c) were observed in BLC group. On the other hand, the lung lesions in BLC+MOL and MOL+BLC groups were significantly lower than that of the BLC group ($P<0.001$). Although lung damage was alleviated in preventive and treatment groups, treatment with MOL before BLC injection was more effective than treatment with MOL after BLC injection (Fig. 3b–d). No
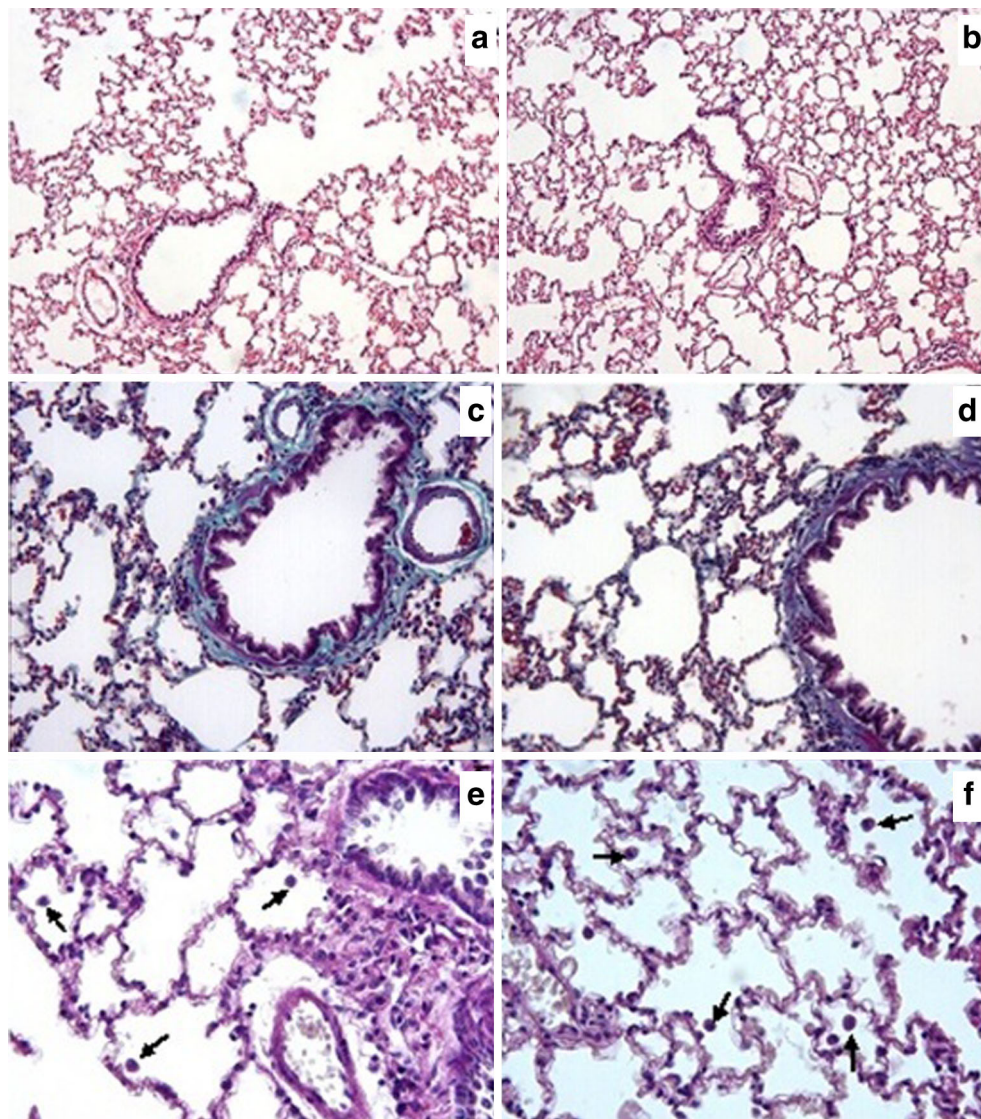
Fig. 1. Histopathological findings in the control (**a**, **c**, **e**) and MOL (**b**, **d**, **f**) groups. **a**, **b** Normal alveoli and interstitial tissue; H&E, ×10. **c**, **d** The view of connective tissue (green staining indicate connective tissue) Masson's trichrome, ×20. **e**, **f** Macrophages in alveolar lumen are observed (*arrows*) PAS, ×40.

significant improvement was observed in the BLC+MOL group in terms of congestion and enlarged alveoli (Fig. 3a).

Other remarkable finding was that many numbers of alveolar macrophage were detected in the alveolar and bronchial lumen in the BLC group with the PAS staining method (Fig. 2d). On the other hand, a number of alveolar macrophages was found to be significantly decreased in BLC+MOL and MOL+BLC groups when compared to the BLC group (Fig. 3e, f; *P*=0.04).

The results of semiquantitative histological scores and number of alveolar macrophages in all the groups were shown in Tables 1 and 2.

Changes in Oxidative Stress Parameters   *MDA content.* The MDA levels reflecting lipid peroxidation end-products were increased by the exposure to BLC compared to the control group (130.46±12.54 *vs*. 50.89±14.71 nmol/g; *P*<0.0001). Increased tissue MDA levels were significantly reduced in the MOL+BLC (but not in the BLC+MOL) group when compared to the group treated with BLC alone (94.27±22.38 nmol/g; *P*=0.002).

SOD. Although SOD in the BLC group did not reach a statistically significant level when compared to the control group, this was found to have a tendency to decrease (Table 3).
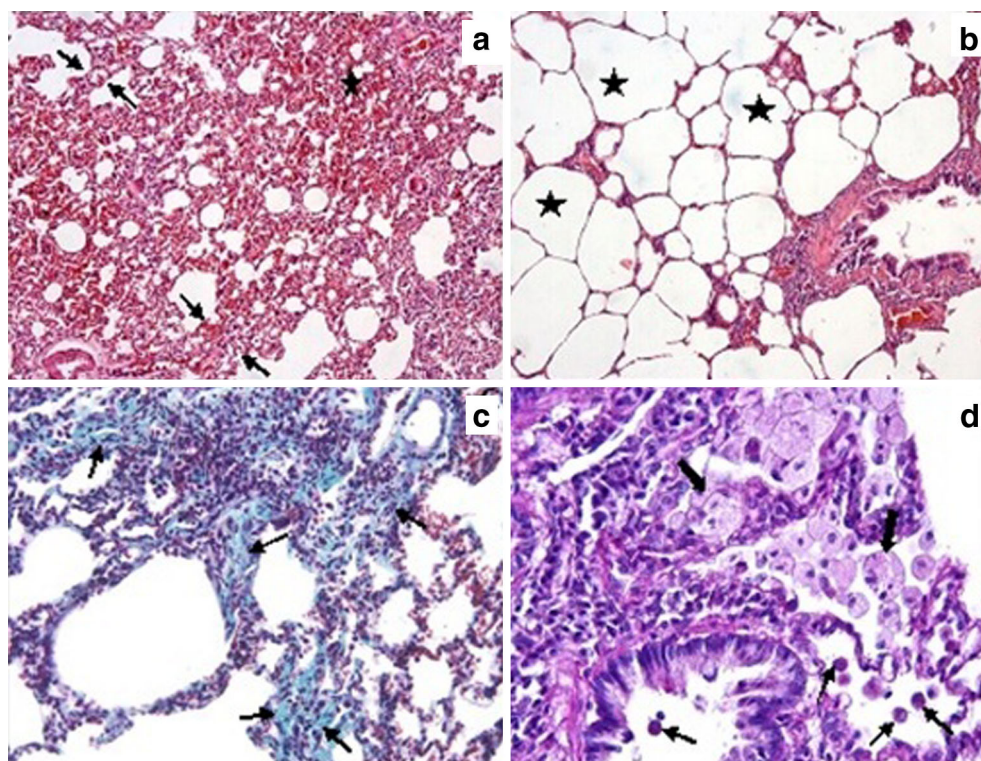
Fig. 2. Histopathological findings in the BLC group; **a** congestion of the parenchyma (*asterisk*) and thickening of interalveolar septum are evident (*arrows*); H&E, ×10. **b** Mark of the enlargement of alveolar walls (*asterisks*); H&E, ×10. **c** Dense in the bundles of collagen are recognized as green (*arrows*) Masson's trichrome, ×20. **d** *Thick arrows* accumulation of lipid-laden macrophages, *thin arrows* alveolar macrophages in alveolar and bronchial lumen PAS; ×40.

CAT. As shown in Table 3, the activity of CAT in the lung tissue was reduced by treatment of BLC; however, the reduction was not significant when compared to the control group (9.67±1.51 *vs.* 12.45±2.32 k/g protein; $P>0.05$). There was an increase in the reduced CAT activity in the MOL+BLC and BLC+MOL groups when compared to the group treated with BLC alone. However, this increase was statistically significant only in the BLC+MOL group compared to the group treated with BLC alone (14.98±3.36 *vs.* 9.67±1.51 k/g protein; $P=0.0001$).

GPx. Although GPx in the BLC group did not reach a statistically significant level when compared to the control group, this was found to have a tendency to decrease (11.54±2.60 *vs.* 12.77±3.31 U/mg; $P>0.05$). Otherwise, there was a slight but insignificant change in groups treated with MOL before and after BLC injection (12.23±2.49 and 11.80±1.35, respectively; $P>0.05$) (Table 3).

GSH. The level of GSH content in lung tissue was reduced by the treatment of BLC, and the reduction was significant compared to the control group [5.59(4.72–7.20) *vs.* 8.65(7.23–11.47) μmol/g tissue; $P<0.0001$]. As shown in Table 3, there were increases in the reduced GHS content

in the MOL+BLC and BLC+MOL groups compared to the group treated with BLC alone. However, this increase was statistically significant only in MOL+BLC group compared to the group treated with BLC alone [7.91(5.97–9.95) *vs.* 5.59 (4.72–7.20)μmol/g tissue; $P<0.0001$].

MPO. MPO activity was increased by BLC exposure when compared to the control groups (66.39±22.04 *vs.* 41.00±9.20 mU/g; $P=0.015$). As shown in Table 3, although MPO in the BLC+MOL and MOL+BLC groups did not reach a statistically significant level when compared to the BLC group, they were found to have a tendency to decrease.

TAS. As shown in Table 3, BLC administration leads to a decrease in TAS level in the lung tissue [0.82(0.76–0.94)mmol trolox equiv/L], and this reduction was significantly reversed by treatment with MOL before and after BLC administration (1.03 (0.53–1.26) and 1.07 (0.80–1.81)mmol trolox equiv/L, respectively; $P<0.0001$).

TOS. The level of TOS in the lung tissue was increased by the treatment of BLC, and this increment was significant compared to the controls (14.11±3.1 *vs.* 8.35± 2.33 mmol H_2O_2 equivalent/L; $P<0.0001$). Increased
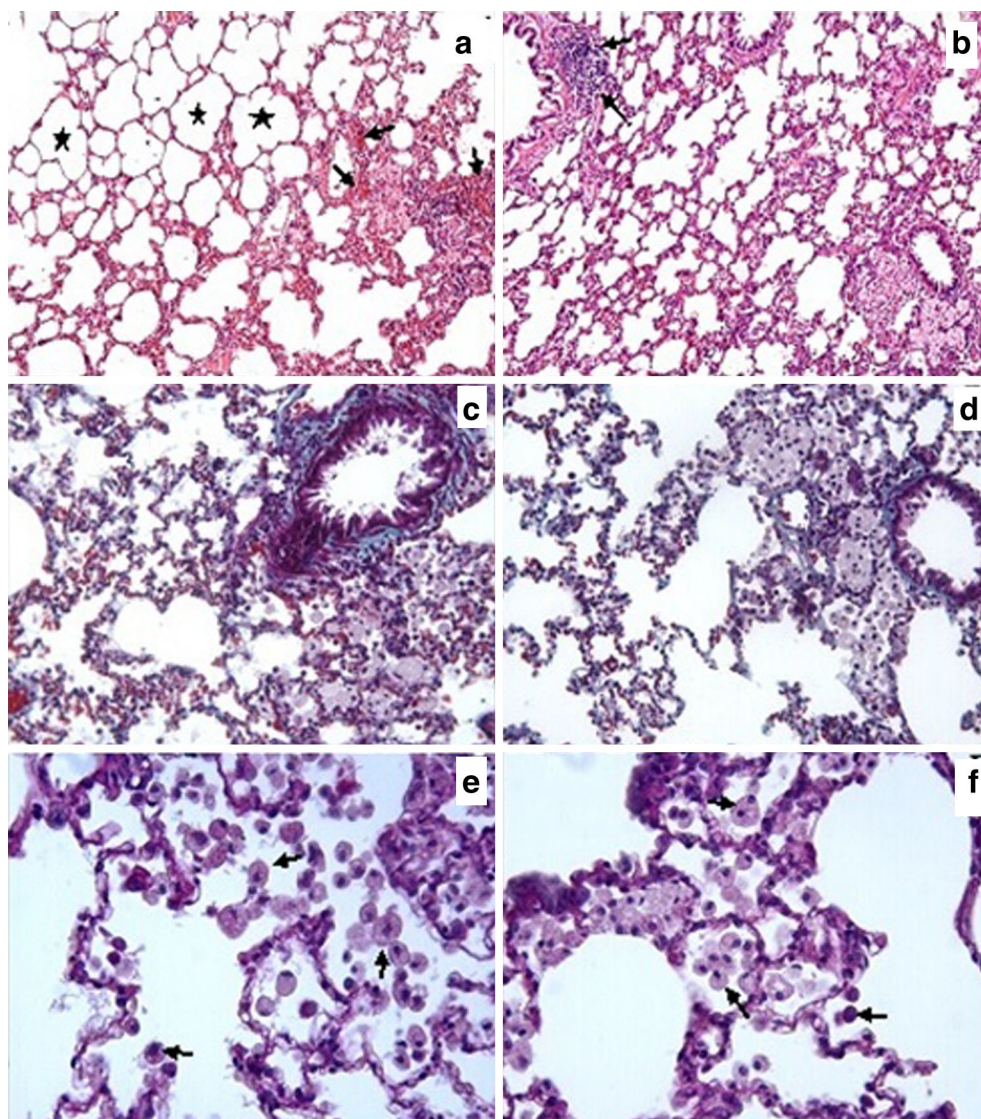
Fig. 3. Histopathological findings in the BLC+MOL and MOL+BLC groups. BLC+MOL group; **a** congestion (*arrows*) and enlarged alveoli (*asterisks*) are still present; H&E, ×10. MOL+BLC group; **b** the appearance of lung is almost intact except mild inflammation H&E, ×10. BLC+MOL (**c**) and MOL+BLC (**d**) groups; the view of connective tissue is similar to control group Masson's trichrome, ×20. BLC+MOL (**e**) and MOL+BLC (**f**) groups; Alveolar macrophages show alveolar lumen (*arrows*) PAS, ×40.

tissue TOS levels were reduced in the MOL+BLC and BLC+MOL groups when compared to the group treated with BLC alone (Table 3). However, there was only a significant reduction in the MOL+BLC group when compared to the BLC group (9.19 ± 2.52 *vs.* 14.11 ± 3.1 µmol H_2O_2 equivalent/L; $P=0.001$).

OSI. OSI was increased by BLC treatment compared to the control groups (16.91 ± 22.27 *vs.* 7.45 ± 2.43 arbitrary unit; $P<0.0001$). Increased OSI were significantly reduced in the MOL+BLC and BLC+MOL groups compared to the

BLC administration group ($P<0.0001$ and $P=0.002$, respectively; Table 3).

White Blood Cell Count of BAL Fluid

White Blood Cell Count (WBC) in BAL fluid in BLC group [$(1.3\pm0.06)\times10^{6}/mL^{-1}$] significantly increased as compared with control group [$(0.51\pm0.045)\times10^{6}/mL^{-1}$]

Table 1. The Results of Semiquantitative Histological Assessment in All Groups

Parameters	Control	MOL	BLC	BLC+MOL	MOL+BLC
Alveolar congestion	0 (0–1)	0 (0–2)	1 (0–2)[a]	1 (0–2)	0 (0–1)[b]
Enlarged alveoli	0 (0–0)	0 (0–0)	2 (1–3)[a]	1 (1–2)	1 (0–3)[b]
Increase connective tissue	0 (0–0)	0 (0–0)	1 (1–2)[a]	0 (0–1)[b]	0 (0–1)[b,c]
Infiltration	0 (0–1)	0 (0–1)	2 (1–3)[d]	1 (0–2)[e]	1 (0–1)[e,c]
The thickness of alveolar wall	0 (0–0)	0 (0–0)	2 (0–2)[a]	1 (0–1)[b]	0 (0–2)[b]

Data were presented as median (min–max)
[a] Significant increase (P=0.0001) vs. control
[b] Significant decrease (P=0.0001) vs. BLC
[c] Not significant (P>0.05) vs. BLC+MOL
[d] Significant increase (P=0.0002) vs. control
[e] Significant decrease (P=0.0002) vs. BLC

and MOL group $[(0.53\pm0.02)\times10^6/mL^{-1}]$ ($P<0.05$). WBC in BAL fluid in BLC+MOL group $[(0.64\pm0.09)\times10^6/mL^{-1}]$ and MOL+BLC group $[(0.65\pm0.04)\times10^6/mL^{-1}]$ significantly decreased as compared with BLC group $[(1.3\pm0.06)\times10^6/mL^{-1}$ ($P<0.05$)]. However, there was no significant difference between the groups in the bottom of the cell types of WBC (data not shown). These results indicated that administration of MOL before and after BLC instillation alleviated the infiltration of leukocyte in the lungs.

DISCUSSION

Nowadays, pulmonary fibrosis is admittedly resulting from the recurrent epithelial damage and apoptosis followed by insufficient re-epithelialization and aberrant wound healing [28, 29]. Essential to the abnormal fibrotic reaction are transforming growth factor (TGF), a major profibrotic mediator, and myofibroblasts, the key cell type of overdone extracellular matrix deposition and distorted lung architecture, which constitute the typical features of IPF [28]. However, the BLC-induced lung fibrosis animal model is widely used for researches of new treatment and pathogenesis of IPF. In this model, it is used as a single intratracheal dose of the drug during the first 7 days to induce an inflammatory response [30] and increase the epithelial

apoptosis [31], closely mimicking acute lung injury (ALI). Inflammatory response continues for 14 days. Subsequently, the inflammation resolves, and fibrosis are detected during the following transitional period of 3 days. The late (fibrotic) stage persists for 3–4 weeks following BLC administration and is characterized by intense deposition of extracellular matrix, resulting in the fibrotic tissue [32].

In the current study, BLC caused significant lung injury demonstrated with histopathological findings such as intense inflammation characterized by accumulation of alveolar macrophage, intense leukocyte migration not only in peribronchial and perivascular areas but also in the interstitial and intrabronchial spaces, and dense bundles of collagen deposition. Moreover, enlarged alveoli, thickening of interalveolar septum, and increase in connective tissue were observed in BLC-treated rats. Also, BLC administration caused the prominent TOS, a novel index oxidative stress, MDA, an end-product of lipid peroxidation, and MPO activity, indicating the increased PMN activity, in the lung tissues. In addition, OSI, which is a novel and very important index of oxidative stress, was higher in the BLC group than the all other groups. These findings seem to be related to the induction of lung injury, consistent with other studies which utilized BLC-induced lung fibrosis models [7, 28, 29, 32]. The BLC-induced lung damage comprises, as a primary event, the generation

Table 2. The Results of Number of Alveolar Macrophage in All Groups

Parameters	Control	MOL	BLC	BLC+MOL	MOL+BLC
Number of alveolar macrophage	5 (0–15)	5 (0–16)	12 (2–95)[a]	10 (2–42)[b]	9 (3–18)[b,c]

Data were presented as median (min-max)
[a] Significant increase (P=0.0001) vs. control
[b] Significant decrease (P=0.0001) vs. BLC
[c] Not significant (P>0.05) vs. BLC+MOL

Table 3. Comparison of the Tissue Oxidative Stress Parameters and MPO Activity Among the Study Groups

Groups	MDA (nmol/g tissue)	SOD (U/g protein)	CAT (K/g protein)	GPX (U/mg protein)	GSH (micromole/g tissue)	MPO (mU/g prot)	TOS (µmol H_2O_2Eq/L)	TAS (mmolTrolox Eq/L)	OSI (arbitrary unit)
Control	50.89±14.71	1.13±0.21	12.45±2.32	12.77±3.31	8.65 (7.23–11.47)	41.00±9.20	8.35±2.33	1.13 (0.93–1.47)	7.45±2.43
MOL	69.25±10.02	1.22±0.29	12.10±3.51	14.32±2.43	7.02 (5.18–9.74)	37.46±9.54	9.42±2.17	1.22 (1.03–1.33)	7.7±1.93
BLC	130.46±12.54[a]	1.03±0.15[b]	9.67±1.51[c]	11.54±2.60[b]	5.59 (4.72–7.20)[d]	66.39±22.04[e]	14.11±3.1[a]	0.82 (0.76–0.94)[f]	16.91±2.27[g]
BLC+MOL	129.74±12.25	1.07±0.19	14.98±3.36	11.80±1.35	6.27 (4.95–8.07)	62.92±13.62	12.44±1.83	1.07 (0.80–1.81)	11.19±2.70
MOL+BLC	94.27±22.38	1.04±0.16	11.36±2.14	12.232.49	7.91 (5.97–9.95)	54.28±12.37	9.19±2.52	1.03 (0.53–1.26)	8.69±2.43

Data were presented as mean ± SEM and median (min–max)

[a] Significant increase ($P<0.05$) vs. all groups except BLC+MOL

[b] Not significant ($P>0.05$) vs. all groups

[c] Significant decrease($P<0.05$) vs. BLC+MOL group

[d] Significant decrease ($P<0.05$) vs. control and MOL+BLC groups

[e] Significant increase ($P<0.05$) vs. control and MOL groups

[f] Significant decrease ($P<0.05$) vs. all groups

[g] Significant increase ($P<0.05$) vs.all groups

of oxidant species by iron-dependent mechanism [33]. Further damage is probably elicited by augmented amounts of reactive oxygen space (ROS) and reactive nitrogen space produced by activated inflammatory cells recruited into the damaged lung induced by BLC administration [7].

In organism, the levels of antioxidants and free radicals, at least, should be in balance to prevent oxidative stress [34]. Therefore, in this study, the levels of oxidative stress indicators were evaluated. In addition to the BLC-provoked inflammation and dense collagen deposition (Fig. 2), we showed that BLC also induced a significant reproduction in lipid peroxide levels accompanied by significantly reduced levels of GSH compared to the control group. Depending on the increases of oxidant production and lipid peroxidation, GSH levels were decreased. Because GSH is necessary for the prevention of thiol and other nucleophilic groups in proteins from the free oxygen radicals, the amount of intracellular GSH is the most important factor in determining the degree of BLC-induced lung damage [35–37]. In the present study, attenuation of GSH concentration after BLC administration was reversed by MOL (especially in MOL+BLC group) treatment (Table 3). Furthermore, it was demonstrated that MOL administration, both before and after BLC administration, increased the level of TAS which was reduced by BLC.

MOL decarboxylases enzymatically to form 3-morpholinosyndnonimine (SIN-1) which spontaneously release NO in the liver [13]. NO is a substantial endogenous regulatory particle, contained in both pro-inflammatory and anti-inflammatory processes in the lung. In the experimental models, NO reduced lung parenchyma damage, alveolar macrophage and neutrophil function, and the transendothelial migration of activated neutrophils during acute lung damage [38–40]. In another animal study, it has been shown that NO donor (S-nitroso-acety penicillamine like MOL) decreases neutrophil adhesion in both lung and peritoneum during peritonitis [41]. Similar to those previous studies, in the present study, accumulation of alveolar macrophage in the alveolar and bronchial lumen was significantly reduced by treatment of MOL before and after BLC administration. Also, the account of neutrophils in BAL fluid that has been increased by BLC was reversed by MOL. It is reported that the beneficial effects of inhaled NO on ALI include inhibition of NF-κB which was playing an important role in inflammation and preserving the alveolar capillary membrane wholeness [39, 40, 42]. In the current study, because of the limited facilities, NF-κB determination was not studied. Nevertheless, because it was investigated in the previous studies [39, 40], it seems to be related that MOL could have improved in the BLC-

better to indicate that MOL downgrades developed fibrosis. Also, especially TGF, which is an important pro-fibrotic mediator and pro-inflammatory cytokines such as TNF-α, IL-1, and IL-6 in BAL fluid have not been studied on. Another limiting aspect of this study is related to the agent (MOL) which was applied. Because MOL is an NO donor, levels of lung tissue NO and nitrite/nitrate, an index of NO production, must have been evaluated. However, some previous studies showed that NO are involved in the pathogenesis of pulmonary inflammation and fibrosis [48–51]. In addition, in one of those studies [7], it has been shown that NO-synthesized inhibitor agent prevented pulmonary inflammation and fibrosis. Therefore, the presence of a group of the NO-synthesized inhibitor agent that was applied would be more rational.

In conclusion, findings of the present study showed for the first time that MOL, with its potent free radical scavenging, antioxidant, anti-inflammatory, and anti-fibrotic properties, seems to be a highly promising agent not only in preventing but also in treatment BLC-induced lung inflammation and fibrosis. However, further studies are required to evaluate the role of different doses of MOL in the prevention and the treatment of lung fibrosis. After clinical and experimental trials, including different treatment dosages, MOL, which was widely used as antianginal agent and have no important side-effects, could be considered in the treatment of IPF in the future.

REFERENCES

1. Raghu, G., H.R. Collard, J.J. Egan, F.J. Martinez, J. Behr, K.K. Brown, T.V. Colby, J.F. Cordier, K.R. Flaherty, J.A. Lasky, *et al.* 2011. An official ATS/ERS/JRS/ALAT statement: Idiopathic pulmonary fibrosis: Evidence-based guidelines for diagnosis and management. *American Journal of Respiratory and Critical Care Medicine* 183: 788–824.
2. Gross, T.J., and G.W. Hunninghake. 2001. Idiopathic pulmonary fibrosis. *New England Journal of Medicine* 345: 517–525.
3. Dedon, P.C., and I.H. Goldberg. 1992. Free-radical mechanisms involved in the formation of sequence-dependent bistranded DNA lesions by the antitumor antibiotics bleomycin, neocarzinostatin, and calicheamicin. *Chemical Research in Toxicology* 5: 311–332.
4. Cottin, V. 2013. The role of pirfenidone in the treatment of idiopathic pulmonary fibrosis. *Respiratory Research* 14(1): 5. doi:10.1186/1465-9921-14-S1-S5.
5. Mata, M., A. Ruíz, M. Cerdá, M. Martinez-Losa, J. Cortijo, F. Santangelo, A. Serrano-Mollar, A. Llombart-Bosch, and E.J. Morcillo. 2003. Oral *N*-acetylcysteine reduces bleomycin-induced lung damage and mucin Muc5ac expression in rats. *European Respiratory Journal* 22(6): 900–905.
6. Sogut, S., H. Ozyurt, F. Armutcu, *et al.* 2004. Erdosteine prevents bleomycin-induced pulmonary fibrosis in rats. *European Journal of Pharmacology* 494: 213–220.
7. Yildirim, Z., Y. Turkoz, M. Kotuk, *et al.* 2004. Effects of aminoguanidine and antioxidant erdosteine on bleomycin-induced lung fibrosis in rats. *Nitric Oxide* 11: 156–165.
8. Yildirim, Z., M. Kotuk, H. Erdogan, M. Iraz, M. Yagmurca, I. Kuku, and E. Fadillioglu. 2006. Preventive effect of melatonin on bleomycin-induced lung fibrosis in rats. *Journal of Pineal Research* 40: 27–33.
9. Iraz, M., H. Erdogan, M. Kotuk, M. Yagmurca, T. Kilic, H. Ermis, E. Fadillioglu, and Z. Yildirim. 2006. Ginkgo biloba inhibits bleomycin-induced lung fibrosis in rats. *Pharmacological Research* 53: 310–316.
10. Akgedik, R., S. Akgedik, H. Karamanli, S. Uysal, B. Bozkurt, D. Ozol, F. Armutcu, and Z. Yildirim. 2012. Effect of resveratrol on treatment of bleomycin-induced pulmonary fibrosis in rats. *Inflammation* 35(5): 1732–1741.
11. Ermis, H., H. Parlakpinar, G. Gulbas, N. Vardi, A. Polat, A. Cetin, T. Kilic, and Z.A. Aytemur. 2013. Protective effect of dexpanthenol on bleomycin-induced pulmonary fibrosis in rats. *Naunyn-Schmiedeberg's Archives of Pharmacology.* doi:10.1007/s00210-013-0908.
12. Gupta, A., S. Sharma, and K. Chopra. 2008. Reversal of iron-induced nephrotoxicity in rats by molsidomine, a nitric oxide donor. *Food and Chemical Toxicology* 46(2): 537–543.
13. Kukovetz, W.R., and S. Holzmann. 1986. Cyclic GMP as the mediator of molsidomine-induced vasodilatation. *European Journal of Pharmacology* 122: 103–109.
14. Valdivielso, J.M., and R.C. Blantz. 2002. Acute renal failure: Is nitric oxide the bad guy? *Redox Signaling* 4: 925–934.
15. Walder, C.E., C. Thiemermann, and J.R. Vane. 1991. The involvement of endothelium-derived relaxing factor in the regulation of renal cortical blood flow in the rat. *British Journal of Pharmacology* 102: 967–973.
16. Garcia-Criado, F.J., N. Eleno, F. Santos-Benito, *et al.* 1998. Protective effect of exogenous nitric oxide on the renal function and inflammatory reaction in a model of ischemia-reperfusion. *Transplantation* 66: 982–990.
17. Chander, V., and K. Chopra. 2005. Renal protective effect of molsidomine and L-arginine in ischemia-reperfusion induced injury in rats. *Journal of Surgical Research* 128(1): 132–139.
18. Marios, A.M., and V. Aidinis. 2011. Modeling pulmonary fibrosis with bleomycin. *Current Opinion in Pulmonary Medicine* 17: 355–361.
19. Colak, C., and H. Parlakpınar. 2012. Hayvan Deneyleri: *In vivo* Denemelerin Bildirimi: ARRIVE Kılavuzu-Derleme. *Journal of Turgut Ozal Medical Center* 19(2): 128–131.
20. Uchiyama, M., and M. Mihara. 1978. Determination of malondehyde precursor in tissues by tiobarbituric acid test. *Analytical Biochemistry* 34: 271–278.
21. Sun, Y., L. Oberley, and Y. Li. 1988. A simple method for clinical assay of superoxide dismutase. *Clinical Chemistry* 34: 497–500.
22. Aebi, H. 1974. Catalase. In *Methods of enzymatic analysis*, ed. H.U. Bergmeyer, 673–677. New York: Academic.
23. Paglia, D.E., and W.N. Valentine. 1967. Studies on the quantitative and qualitative characterization of erythrocyte glutathione peroxidase. *Journal of Laboratory and Clinical Medicine* 70: 158–170.
24. Ellman, G.L. 1959. Tissue sulfhydryl groups. *Archives of Biochemistry and Biophysics* 82: 70–77.
25. Wei, H., and K. Frenkel. 1993. Relationship of oxidative events and DNA oxidation in Sencar mice to *in vivo* promoting activity of phorbol ester-type tumor promoters. *Carcinogenesis* 14: 1195–1201.

26. Erel, O. 2004. A novel automated direct measurement method for total antioxidant capacity using a new generation, more stable ABTS radical cation. *Clinical Biochemistry* 37: 277–285.

27. Erel, O. 2005. A new automated colorimetric method for measuring total oxidant status. *Clinical Biochemistry* 38: 1103–1111.

28. Coward, W.R., G. Saini, and G. Jenkins. 2010. The pathogenesis of idiopathic pulmonary fibrosis. *Therapeutic Advances in Respiratory Disease* 4: 367–388.

29. Harari, S., and A. Caminati. 2010. IPF: New insight on pathogenesis and treatment. *Allergy* 65: 537–553.

30. Chaudhary, N.I., A. Schnapp, and J.E. Park. 2006. Pharmacologic differentiation of inflammation and fibrosis in the rat bleomycin model. *American Journal of Respiratory and Critical Care Medicine* 173: 769–776. 352006.

31. Mungunsukh, O., A.J. Griffin, Y.H. Lee, and R.M. Day. 2010. Bleomycin induces the extrinsic apoptotic pathway in pulmonary endothelial cells. *American Journal of Physiology-Lung Cellular and Molecular Physiology* 298: 696–703.

32. Mouratis, M.A., and V. Aidinis. 2011. Modeling pulmonary fibrosis with bleomycin. *Current Opinion in Pulmonary Medicine* 17: 355–361.

33. Sleijfer, S. 2001. Bleomycin-induced pneumonitis. *Chest* 120: 617–624.

34. Valko, M., D. Leibfritz, J. Moncol, M.T. Cronin, M. Mazur, and J. Telser. 2007. Free radicals and antioxidants in normal physiological functions and human disease. *The International Journal of Biochemistry & Cell Biology* 39: 44–84.

35. Cortijo, J., M. Cerda-Nicolas, A. Serrano, G. Bioque, J.M. Estrela, F. Santangelo, *et al*. 2001. Attenuation by oral *N*-acetylcysteine of bleomycin-induced lung injury in rats. *European Respiratory Journal* 17: 1228–1235.

36. Ross, D. 1988. Glutathione, free radicals and chemotherapeutic agents. *Pharmacology and Therapeutics* 37: 231–249.

37. Venkatesan, N., V. Punithavathi, and G. Chandrakasan. 1997. Curcumin protects bleomycin-induced lung injury in rats. *Life Sciences* 61: L51–L58.

38. Kang, J.L., W. Park, I.S. Pack, H.S. Lee, M.J. Kim, C.M. Lim, *et al*. 2002. Inhaled nitric oxide attenuates acute lung injury via inhibition of nuclear factor-kappa B and inflammation. *Journal of Applied Physiology* 92: 795–801.

39. Hong-ping, X.I.A., H. Guo-ying, Z.H.U. Jian-xing, and S.U.N. Bo. 2008. Effect of inhalation of nebulized NO donor substance on acute hypoxic lung injury in newborn piglets. *Chinese Medical Journal* 121(17): 1622–1626.

40. Kinsella, J.P., T.A. Parker, and H. Galan. 1997. Effects of inhaled nitric oxide on pulmonary edema and lung neutophil accumulation in severe experimental hyaline membrane disease. *Pediatric Research* 41(Pt 1): 457–463.

41. Fukatsu, K., H. Saito, I. Han, *et al*. 1998. Nitric oxide donor decreases neutrophil adhesion in both lung and peritoneum during peritonitis. *Journal of Surgical Research* 74: 119–124.

42. Cao, L., L.L. Qian, Y.R. Zhu, C.B. Guo, X.H. Gong, and B. Sun. 2003. Regulation of activity of nuclear factor-kappa B and activator protein-1 by nitric oxide, surfactant and glucocorticoids in alveolar macrophages from piglets with acute lung injury. *Acta Pharmacologica Sinica* 24: 1316–1323.

43. Bentli, R., H. Parlakpinar, A. Polat, *et al*. 2013. Molsidomine prevents cisplatin-induced hepatotoxicity. *Archives of Medical Research* 44: 521–528.

44. Disli, O.M., E. Sarihan, M.C. Colak, *et al*. 2013. Effects of molsidomine against doxorubicin-induced cardiotoxicity in rats. *European Surgical Research* 51: 79–90.

45. Grisham, M.B. 1995. Interaction between nitric oxide and superoxide: role in modulating leukocyte adhesion in the postischemic microvasculature. *Transplantation Proceedings* 27: 2842.

46. Clancy, R.M., J. Leszczynska-Piziak, and S.B. Abramson. 1992. Nitric oxide, an endothelial cell relaxation factor, inhibits neutrophil superoxide anion production via a direct action on the NADPH oxidase. *Journal of Clinical Investigation* 90: 1116.

47. Aoki, F., M. Kurabayashi, Y. Hasegawa, and I. Kojima. 2005. Attenuation of bleomycin-induced pulmonary fibrosis by follistatin. *American Journal of Respiratory and Critical Care Medicine* 172: 713–720.

48. Kakugawa, T., H. Mukae, T. Hayashi, H. Ishii, K. Abe, T. Fujii, *et al*. 2004. Pirfenidone attenuates expression of HSP47 in murine bleomycin-induced pulmonary fibrosis. *European Respiratory Journal* 24: 57–65.

49. Peters, H., *et al*. 2003. NO mediates antifibrotic actions of L-arginine supplementation following induction of anti-thy1 glomerulonephritis. *Kidney International* 64: 509–518.

50. Giri, S.N., I. Biring, T. Nguyen, *et al*. 2002. Abrogation of bleomycin induced lung fibrosis by nitric oxide synthase inhibitor, aminoguanidine in mice. *Nitric Oxide* 7: 109–118.

51. Chen, X.L., W.B. Li, A.M. Zhou, *et al*. 2003. Role of endogenous peroxynitrite in pulmonary injury and fibrosis induced by bleomycin A5 in rats. *Acta Pharmacologica Sinica* 24: 697–702.